

Article

A Numerical Study on the Exergy Performance of a Hybrid Radiant Cooling System in an Office Building: Comparative Case Study and Analysis

Jiying Liu ¹ , Meng Su ¹, Nuodi Fu ^{2,3} and Moon Keun Kim ^{4,*} ¹ School of Thermal Engineering, Shandong Jianzhu University, Jinan 250101, China² School of Architecture, Southeast University, Nanjing 210096, China³ School of Architecture, University of Liverpool, Liverpool L69 7ZX, UK⁴ Department of Built Environment, Oslo Metropolitan University, 0130 Oslo, Norway

* Correspondence: moon.kim@oslomet.no; Tel.: +47-67-23-65-57

Abstract: This research investigated the exergy enhancement performance of a hybrid radiant cooling system adapting to a hot and humid summer conditions through comparative case studies and analyses. This study suggested three cooling systems: a general all-air system (AAS), a conventional radiant cooling system (CRCS), and a hybrid radiant cooling system (HRCS). As a case study, an office building with cooling systems was examined in the summer season in four different cities: Beijing, Shanghai, Chengdu, and Guangzhou, China. This study utilized the building energy performance simulation program to analyze the cooling loads of office space in a building with numerical approaches. The comparison analysis using the four different weather datasets showed simple and rational exergy efficiency and the overall impact ratio. According to the results, the ambient conditions, i.e., the surrounding temperature and the humidity ratio, significantly impacted the cooling systems' exergy efficiency ratio. On the basis of the calculated energetic and exergetic performance, the HRCS had a higher exergy efficiency and a higher overall impact ratio. The HRCS system released an additional 20–30% of cooling output, and it could adapt well in extreme hot and humid weather conditions compared to the AAS and the CRCS system. The overall cooling impact ratio of the HRCS with an airbox convector was approximately 185% higher than that of the AAS and 8.5% higher than that of the CRCS. This study can provide the design references for the hybrid radiant cooling system and other cooling systems in hot and humid summer conditions.

Keywords: comparative study; exergy analysis; cooling systems; hot and humid climates



Citation: Liu, J.; Su, M.; Fu, N.; Kim, M.K. A Numerical Study on the Exergy Performance of a Hybrid Radiant Cooling System in an Office Building: Comparative Case Study and Analysis. *Buildings* **2023**, *13*, 465. <https://doi.org/10.3390/buildings13020465>

Academic Editor: Fabrizio Ascione

Received: 21 November 2022

Revised: 3 February 2023

Accepted: 7 February 2023

Published: 8 February 2023



Copyright: © 2023 by the authors. Licensee MDPI, Basel, Switzerland. This article is an open access article distributed under the terms and conditions of the Creative Commons Attribution (CC BY) license (<https://creativecommons.org/licenses/by/4.0/>).

1. Introduction

Energy consumption in buildings is mainly responsible for climate change and global warming because the building sector emits about one-third of the total amount of global carbon dioxide (CO₂) [1,2]. In the building sector, heating, ventilation, and air-conditioning (HVAC) systems are responsible for the majority of the building energy consumption. In particular, global warming has affected the rise in cooling loads in hot and humid climates. Low-exergy technologies that have a high-temperature cooling system, e.g., radiant cooling systems [3,4], could minimize the actual environmental impact and maximize the energy efficiency of the systems due to the minimization of the exergy released and the CO₂ emissions [5,6].

Many studies have illustrated the exergy performance of space heating and cooling systems in buildings [7,8]. The studies described that an exergy-based analysis strategy could represent a high-performance system and optimize the exergy efficiency. Moreover, the exergy-based analysis accurately articulates energy source quality and flow [8,9]. The exergetic approach illustrates a better understanding of our surrounding built environment and the exergy flow for cooling and heating in buildings, as well as how exergy

is constructed or deconstructed in the process [10]. This research newly investigates the exergy enhancement performance of a hybrid radiant cooling system to present the exergy potential and efficiency compared to three different cooling systems, adapting to a local environment as comparative analysis.

It is well known that the conventional radiant cooling system (CRCS) has limited adaptation to surrounding hot and humid conditions due to high air vapor condensation risk on the surface of a radiant cooling panel when unexpected humidity occurs, such as when opening windows or through the moisture generation of occupants. Moreover, it faces difficulty with increasing cooling outputs in extreme weather conditions. Recently, a hybrid radiant cooling system (HRCS) was newly designed, adapted to the hot and humid climate [11–13]. The novel HRCS comprised two units—a CRCS and an airbox convector. The major benefits of this system are that the HRCS can reduce vapor condensation risks on the radiant cooling panel surface due to dehumidification and the adjusted surface temperature using an airbox convector. Moreover, the HRCS can simplify space zoning for cooling in an occupied area due to adjusted air movement and directivity using an airbox convector, and it can improve indoor air quality due to using the air filters in an airbox convector [14].

Energy balance processing has been commonly used to investigate the calculation of energy load and efficiency and performance of the HRCS to adapt to hot and humid summer conditions; however, the balance methodology does not indicate the source's energy quality and availability. Recently, exergy analysis combined the two major laws of thermodynamics applied to reflect the coupling of both energy potential and availability [7,15], e.g., using a conventional boiler in a heating center [16] and a novel desiccant cooling system [17]. According to exergy studies, exergy evaluation is defined by the value inherent in heat fluxes denoted throughout gradients of temperature difference [10,18]. Small temperature differences, hence, can minimize exergetic destruction or entropy generation and maximize energy reversibility. Therefore, the high-temperature cooling and low-temperature heating system minimizes the energetic value and the actual environmental impact of the systems [19,20]. For example, a fossil-fuel boiler releases high-temperature energy sources in the combustion process and generates high entropy [21]. However, a low-temperature heating and high-temperature cooling system with a heat pump system can use low-exergetic-energy sources, minimize entropy generation, and utilize energy reversibility with the least energy source added [22,23]. In the end, these leading approaches can improve exergy efficiency and reduce the actual environmental impact of systems [24,25].

Therefore, this study explored the energy and exergy potential performance analyses of a hybrid radiant cooling system compared with three cooling systems adapted to hot and humid summer conditions in four major cities, Beijing, Shanghai, Chengdu, and Guangzhou, located in China, as a comparative analysis. Consequently, the performance of each system was evaluated by exergetic approaches.

2. System Description and Methods

2.1. Cooling Systems in a Building

The common HVAC systems with ventilation can be classified into three types in buildings: an all-air system (AAS), a CRCS with air handling unit (AHU), and an HRCS with an AHU [26,27]. An AAS, which is currently very commonly used, supplies an amount of air to deliver fresh air to occupants, as well as heat transfer and cooling in a room [28,29]. Figure 1 presents the conceptual process of an AAS that supplies chilled and dehumidified outdoor air that is mixed with return air to reduce cooling energy loads. The system can simply adjust air volume depending on the thermal loads. However, it also consumes a large amount of electricity for fan energy and releases airflow noise while supplying a large volume of air.

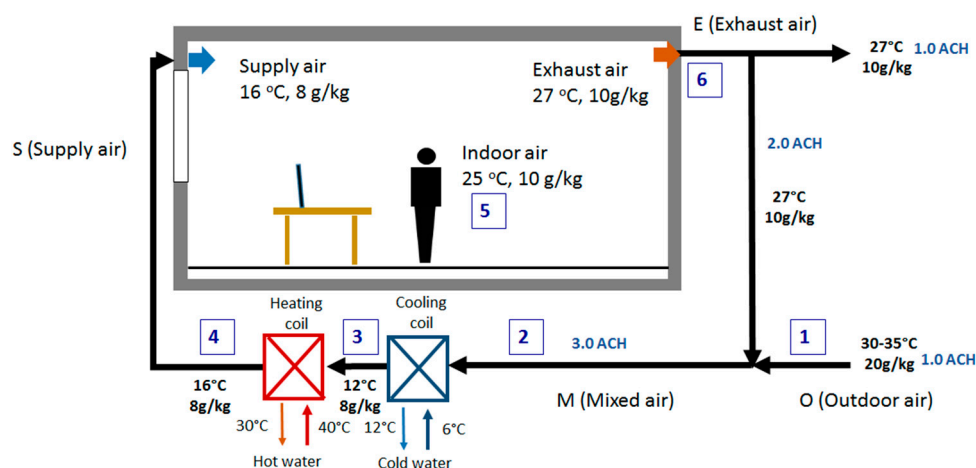


Figure 1. Schematic of the AAS for the cooling, dehumidification, and reheating processes.

A CRCS with an AHU consumes less energy than an AAS [30] because it minimizes the air volume supplied, and the high-temperature cooling system can minimize entropy generation and maximize the coefficient of performance (COP). The system is divided into the air ventilation and cooling tasks by employing radiant cooling panels to deal with the sensible cooling load while utilizing a fresh air supplying system [31,32]. Figure 2 illustrates a schematic of the CRCS with AHU. However, this system has limitations for use in certain places. High internal humidity gains cause moisture condensation on the chilled radiant panel surface. Therefore, the supply air should be dehumidified below 8 g/kg of the humidity ratio in case of internal humidity gains [33,34]. Compared with an AAS, a CRCS has a time delay for activation when cooling in a room [35–37]. Small airflow rates have difficulty improving indoor air quality in a highly polluted zone [30,38,39]. The CRCS also has difficulties adjusting the cooling outcome because a chilled water supply directly passing through the radiant cooling panel causes condensation, especially in hot and humid surrounding conditions [32,40–42]. Most buildings in China use the AAS because China weather conditions are hot and humid in the summer season, and the CRCS is limited to use in a building that combines natural ventilation system and a high infiltration rate with poor air tightness. However, the AAS has been widely used in residential and commercial buildings since it can simply adjust cooling outputs with a variable air volume control system.

Figure 3 shows the schematic HRCS with AHU. A compact air convector and a chilled radiant panel system are connected in series, adjusting and controlling the airflow for cooling and dehumidification in a convector and sensible cooling with a chilled radiant ceiling panel. An airbox convector consists of compact heat exchangers, electric fans, air filter, and a drain tube [43]. During the process in humid indoor conditions higher than a 12 g/kg humidity ratio, the water vapor is condensed in the compact air convector, and the condensed water is drained through a tube [14,44]. The supplied water temperature is increased by 1–2 °C after passing through the airbox unit. The system can simply adjust actual cooling output based on surrounding environments. In general, to prevent moisture condensation on the chilled radiant panel, the supplied water temperature must be around 18 °C and the supplied air should be dehumidified around 8–9 g/kg humidity ratio. However, a HRCS can allow the supplied air to be dehumidified up to 10 g/kg to save cooling energy since an airbox convector can dehumidify the indoor air to reduce moisture condensation risk and to improve thermal comfort in conditions of high internal moisture gain.

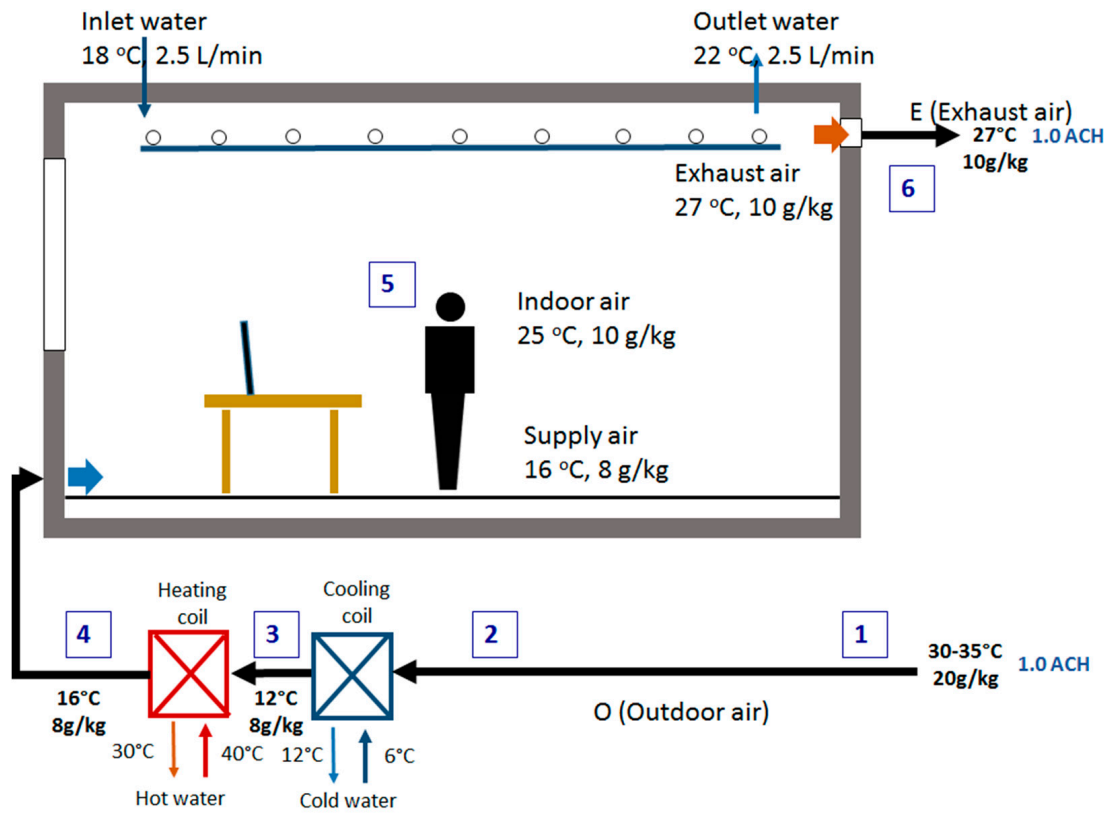


Figure 2. Schematic of the CRCS with AHU.

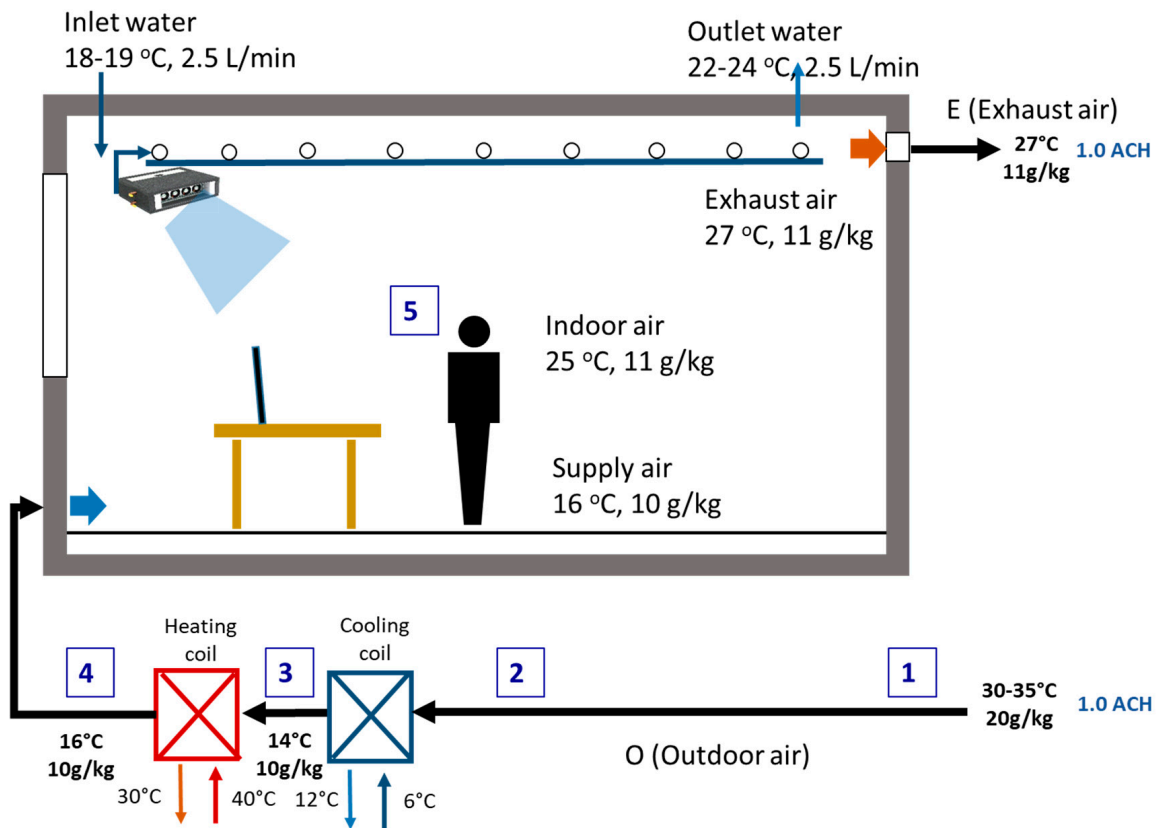


Figure 3. Schematic of the HRCS with AHU.

Figure 4 shows a psychrometric of the three systems. In the figure, the cooling and reheating processes of each system are clearly illustrated as a comparative analysis. We can estimate the quantitative cooling and reheating loads of each system using the psychrometric. However, the psychrometric analysis has a limitation in presenting exergetic performance. Actually, entropy generation and the energy reversibility utilized in the cooling and reheating processes affect the exergy performance. The psychrometric can reflect energy quantitatively but does not provide qualitative analysis.

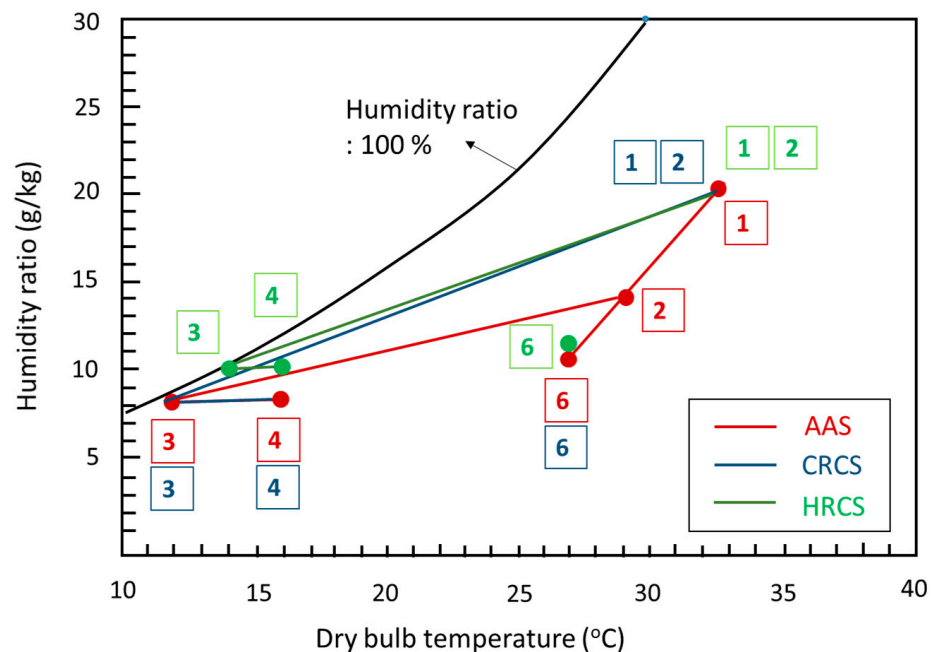


Figure 4. Psychrometric of the AAS, CRCS, and HRCS system.

2.2. Weather and Building Characteristics as Case Studies in China

This study selected four local China weather conditions, Beijing (northern China), Shanghai (southeastern China), Chengdu (northwestern China), and Guangzhou (southern China), to investigate the acceptable performance for the operation of AAS, CRCS, and HRCS in the hot and humid summer season. Beijing, the capital city of China, is located in northern China, and it has hot and humid summer conditions due to East Asian monsoons. Shanghai is located in the Yangtze River in southeastern China and shows a humid subtropical climate. Chengdu, located in northwestern China, has a humid subtropical climate with high relative humidity in the summer season. Guangzhou, located in southern China, has a hot and humid summer with a high heat index.

Figures 5 and 6 illustrate the weather data (temperature and humidity) in the summer season (June–August) of four local cities in China. These places in the summer season are very hot and humid, requiring entirely high cooling and ventilation loads. The Beijing weather data illustrate high temperature variations between day and nighttime, as well as seasonal changes. Therefore, the temperatures oscillate largely in a day, but relatively lower humidity ratios are shown compared to other cities. The Guangzhou weather data show low temperature differences between daytime and nighttime and small seasonal changes, but high temperature and humidity ratios are illustrated in the overall years. Therefore, we estimated that Guangzhou weather was challenging due to high cooling and dehumidification loads. The Shanghai weather conditions present high temperature and humidity ratios in the summer and autumn seasons and a relatively low temperature and humidity ratio in the spring and winter. The Chengdu weather conditions have a similarity to the Beijing and Shanghai weather conditions.

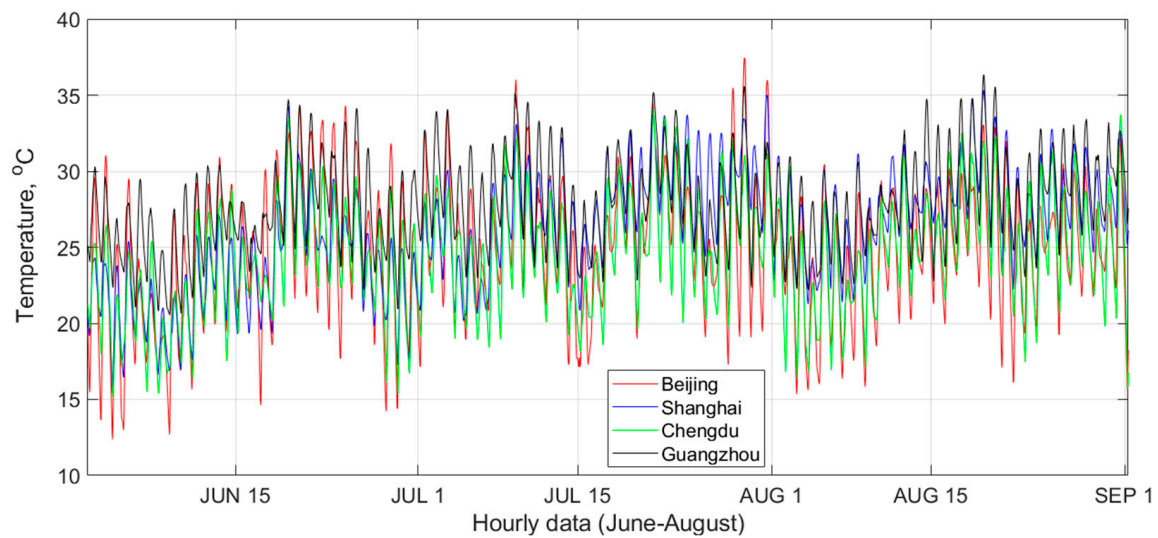


Figure 5. Temperature data for Beijing, Shanghai, Chengdu, and Guangzhou, China.

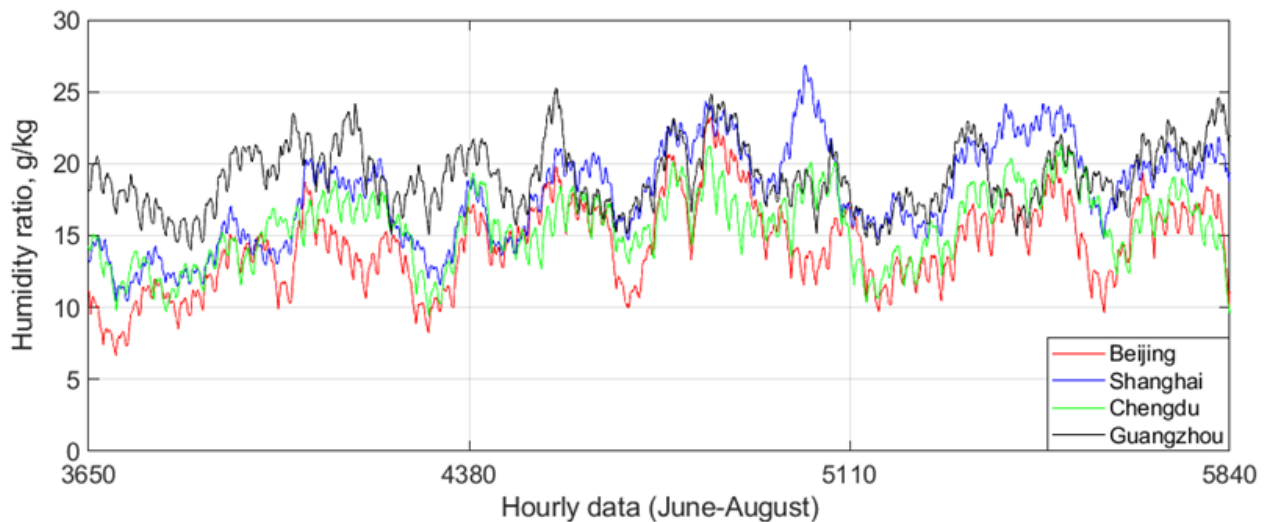


Figure 6. Humidity ratio data for Beijing, Shanghai, Chengdu, and Guangzhou, China.

This study selected a small office space in the four major cities for these case studies, which used a heat pump system for the cooling and air ventilation processes. The container-size office unit was used as a test room to evaluate the cooling and ventilation capacity of an AAS, a CRCS with an AHU, and an HRCS with an AHU. The building wall and window materials were selected and used for a case that was designed as a normal thermal performance case.

The thermal performance of the above systems was simulated using the TRNSYS program [45], which has been widely employed to simulate radiant cooling systems [46]. The multimode building module Type 56 was used to model the dynamic thermal performance by solving the energy balance equations. The heat balance equation considers the change rate of air node thermal energy, building envelope node heat transfer rate, and power out of the indoor heat source node, as shown in Equation (1).

$$c\dot{m}(T_{\text{set}} - T_{\tau}) = \dot{Q}_{\text{surf}} + \dot{Q}_{\text{air}} + \dot{Q}_{\text{inf}} + \dot{Q}_{\text{int}} + \dot{Q}_{\text{solar}}, \quad (1)$$

where c is the specific heat capacity of air in $\text{kJ}/(\text{kg}\cdot\text{K})$, \dot{m} is the mass flow rate in kg/h , T_{set} indicates the indoor cooling set temperature in K , T_{τ} is the indoor air temperature at the time of τ in K , \dot{Q}_{surf} is the radiative and convective gain from the surfaces in kJ/h , \dot{Q}_{air} is

the heat gain due to air entering indoor in kJ/h, Q_{inf} is the infiltration gain in kJ/h, Q_{int} denotes the radiative and convective gains by the internal heat source in kJ/h, and Q_{solar} is the solar radiation gain through the windows in kJ/h.

Table 1 presents the simulation setup of the building model in the software. This is an office room with a floor area of $5\text{ m} \times 3\text{ m}$ and a south-facing window with a window-to-wall ratio of 0.33. Table 2 shows the envelopes' overall heat transfer coefficient (U-values). A recommended supplied air volume flow rate of $43\text{ m}^3/\text{h}$, with 1.0 air changes per hour (ACH), was selected according to international standards for normal air quality [47–49], and the space area of the office room was 14.3 m^2 . This study estimated that two occupants worked in the room.

Table 1. Simulation setting in the office room.

Settings	Values
Volume flow rate (m^3/h)	43
Net floor area (m^2)	15
Indoor air temperature ($^{\circ}\text{C}$)	25
Ventilation rate (h^{-1})	1.0
Infiltration rate (h^{-1})	0.1
Occupant (W)	150×2
Computer (W)	100×2
Lighting (W)	10×2

Table 2. U-values of the building envelope.

Structure	U-Values, $\text{W}/(\text{m}^2 \cdot \text{K})$
Ceiling	0.215
Long wall	0.215
Short wall	0.215
Ground	0.151
Window	1.432

2.3. Energy and Exergy Performance of the Systems

2.3.1. Energy Load Calculation

The energy load for the heat transfer to supply air for cooling is expressed as follows [28,50,51]:

$$\dot{Q} = \dot{m}_{air} \Delta h, \quad (2)$$

where \dot{m}_{air} is the mass flow rate of the supply air (kg/h), and Δh is the enthalpy change value (kJ/kg) in the air cooling and dehumidification process of the heat exchanger with an AHU.

$$\dot{Q}_{total} = \dot{Q}_{sen} + \dot{Q}_{lat}, \quad (3)$$

The total cooling energy load value of air, \dot{Q}_{total} , is calculated from the sum value of the sensible (\dot{Q}_{sen}) and latent (\dot{Q}_{lat}) cooling energy load.

The sensible energy load value of air, \dot{Q}_{sen} , is as follows:

$$\dot{Q}_{sen} = \dot{m}_{air} c_{p,air} \Delta T, \quad (4)$$

The latent energy load value of air, \dot{Q}_{lat} , is as follows:

$$\dot{Q}_{lat} = \dot{m}_{air} h_{fg} \Delta w. \quad (5)$$

The total energy load of the water side is determined from the equation below.

$$\dot{Q}_{water} = \dot{m}_{water} c_{p,water} (T_{out,water} - T_{in,water}), \quad (6)$$

where h_{fg} is the specific enthalpy value of the vaporization of water in kJ/kg, $c_{\text{p,air}}$ is the specific heat capacity value of air in kJ/(kg·K), \dot{m}_{air} is the mass flow rate of air in kg/h, Δw is the change in the humidity ratio of air in kg/kg, ΔT is the temperature change value of air in K, Δh is the change in specific enthalpy in kJ/kg, \dot{m}_{water} is the mass flow rate of water in kg/h, and $c_{\text{p,water}}$ is the specific heat capacity of water in kJ/(kg·K).

The total energy load of AAS for cooling and dehumidification only or for cooling, dehumidification, and reheating is presented as follows:

$$\dot{Q}_{\text{AAS}} = \dot{m}_{\text{sup,air}}(h_{\text{mix,air}} - h_{\text{cooling and dehum}}) + \dot{m}_{\text{sup,air}}c_{\text{p,air}}(T_{\text{reheat}} - T_{\text{c}}). \quad (7)$$

The total energy load of the CRCS with an AHU is shown as follows:

$$\dot{Q}_{\text{CRCS_AHU}} = \dot{m}_{\text{sup,water}}c_{\text{p,water}}(T_{\text{out}} - T_{\text{in}}) + \dot{m}_{\text{sup,air}}(h_{\text{out}} - h_{\text{cooling and dehum}}) + \dot{m}_{\text{sup,air}}c_{\text{p,air}}(T_{\text{reheat}} - T_{\text{c}}). \quad (8)$$

The total energy load of the HRCS with an AHU is shown as follows:

$$\dot{Q}_{\text{HRCS_AHU}} = \dot{m}_{\text{sup,air}}(h_{\text{out}} - h_{\text{c}}) + \dot{m}_{\text{sup,water}}c_{\text{p,water}}(T_{\text{out}} - T_{\text{in}}) + P_{\text{airbox}}. \quad (9)$$

The actual cooling capacities of the AAS, the CRCS with AHU, and the HRCS with AHU are as follows:

$$\dot{Q}_{\text{CC_AAS}} = \dot{m}_{\text{sup,air}}(h_{\text{indoor,air}} - h_{\text{sup,air}}), \quad (10)$$

$$\dot{Q}_{\text{CC_CRCS_AHU}} = \dot{m}_{\text{sup,air}}(h_{\text{indoor,air}} - h_{\text{sup,air}}) + \dot{m}_{\text{sup,water}}c_{\text{p,water}}(T_{\text{out}} - T_{\text{in}}), \quad (11)$$

$$\dot{Q}_{\text{CC_HRCS_AHU}} = \dot{m}_{\text{sup,air}}(h_{\text{indoor,air}} - h_{\text{sup,air}}) + \dot{m}_{\text{sup,water}}c_{\text{p,water}}(T_{\text{out}} - T_{\text{in}}). \quad (12)$$

2.3.2. Exergy Load Calculation

In general, the heat output of a system is a combination of the exergy input (ex_{input}) and anergy input (An_{input} , corresponding to the waste energy) [52,53].

$$\dot{Q}_{\text{ex.an}} = ex_{\text{input}} + An_{\text{input}}. \quad (13)$$

According to the Carnot COP , the heat output is maximized by minimizing the temperature lifting in the thermal process of systems.

$$COP = \frac{\dot{Q}_{\text{max}}}{W_{\text{input}}} = T_{\text{hot}} / (T_{\text{hot}} - T_{\text{cold}}). \quad (14)$$

Exergy presents the energy availability to convert the maximum theoretical work in the energy generated or transferred [52,53]. The exergy is zero when the system's state is in equilibrium with the surrounding environment, the so-called ambient condition [22,52,53]. The ambient condition is defined in terms of the temperature, humidity ratio, pressure, and chemical potentials. In terms of the exergy load evaluation and analysis, the exergy load is classified into two exergy parts, the chemical and physical exergy areas. The chemical exergy is defined by the chemical potential μ_i with the pressure (p_o), temperature (T_o), and chemical potential (μ_o) [53], and the physical exergy is defined by the pressure (p) and temperature (T) of the system. The detailed formulas were illustrated in [22,53,54].

The total specific exergy of a supply air system is shown as follows:

$$ex_{\text{tot}} = ex_{\text{phys}} + ex_{\text{chem}}. \quad (15)$$

The physical exergy of air with humidity is shown as follows [54,55]:

$$ex_{\text{phys.air}} = (C_{p,\text{air}} + \omega C_{p,\text{vapor}}) \left[(T - T_o) - T_o \ln \frac{T}{T_o} \right] + (1 + \tilde{\omega}) R_{\text{air}} T_o \ln \frac{p}{p_o}. \quad (16)$$

The chemical exergy of air with humidity variation is expressed as follows [55,56]:

$$ex_{\text{chem.air}} = R_{\text{air}} T_o \left[(1 + \tilde{\omega}) \ln \frac{1 + \tilde{\omega}_o}{1 + \tilde{\omega}} + \tilde{\omega} \ln \frac{\tilde{\omega}}{\tilde{\omega}_o} \right], \quad (17)$$

where R_{air} is the specific ideal gas constant in J/(kg·K), T_o is the outdoor air temperature in K, ω is the indoor air humidity ratio in kg/kg, $\tilde{\omega}$ is mole fraction ratio, ω_o is the outdoor air humidity ratio in kg/kg, $c_{p,\text{vapor}}$ is the specific heat capacity of water vapor in kJ/(kg·K), and p_o is the outdoor air pressure in Pa.

The liquid water physical specific exergy passing through a ceiling panel for cooling is as follows:

$$ex_{\text{phys.water}} = C_{p,\text{water}} \left[(T - T_o) - T_o \ln \frac{T}{T_o} \right] + v(p - p_o). \quad (18)$$

The chemical exergy of liquid water is shown as follows [54,55]:

$$ex_{\text{chem.water}} = (p - p_{\text{sat}})v - R_w T_o \ln \phi_o, \quad (19)$$

where p_{sat} is the saturated water vapor pressure in Pa, and ϕ_o is the outdoor air relative humidity as a percentage.

To calculate the dynamic total exergy loads with physical and chemical compositions, in this study, a reference environment was used as the actual variable hourly weather data surrounding a building in four major cities, Beijing, Shanghai, Chengdu, and Guangzhou, in China.

Additionally, pump and fan energy represents one of the main parts of an HVAC system. The electric power of the pump and fan energy of the HVAC system is 100% exergy [54]. The calculation of fan and pump power is given as follows [28,51]:

$$P_{\text{fan}} = \dot{V}_{\text{fan}} \Delta p / (3600 \eta_{\text{fan}}), \quad (20)$$

$$P_{\text{pump}} = \dot{V}_{\text{pump}} \Delta p / (3600 \eta_{\text{pump}}), \quad (21)$$

where \dot{V}_{fan} and \dot{V}_{pump} are the air and water volumetric flow rate in m³/h, respectively, Δp represents the total pressure differences in Pa, and η_{fan} and η_{pump} are the fan and pump system efficiencies of units as a percentage, respectively.

2.3.3. Exergy Efficiencies

Exergy analysis shows a methodology to evaluate the impact of a building energy system on the environment [57]. The method accesses a system to present the interactions between building systems, as well as its surroundings, from an exergetic view [57]. Relatively low exergy destruction means low entropy generation; therefore, it can maximize high energy availability in a thermal system [7,11,18]. The reference literature describes the exergy performance efficiencies of a system that is determined as the ratio between the input required or consumed and the output obtained or generated for the exergy in systems [58,59]. In general, two types of exergy efficiencies are defined and explained: "simple or universal" (ψ_{sim}) and "rational and functional" (ψ_{rat}) [22,59]. The mathematical approaches are shown below.

$$\psi_{\text{sim}} = \frac{ex_{\text{out}}}{ex_{\text{in}}}. \quad (22)$$

$$\psi_{\text{rat}} = \frac{ex_{\text{desired,out}}}{ex_{\text{in}}}. \quad (23)$$

Many researchers have investigated the exergy efficiencies using different approaches [11, 54,59]. The simple exergy ratio describes the estimation of differences between the actual involved processes in a system and the ideal performance. The rational exergy ratio presents how much potential is consumed to generate the required output in a system. Generally, exergy losses have been explained with the rational efficiency because the ratio presents both the unconsumed output exergy and the irreversible processes released [22,59].

Simple ratios for different systems are shown as follows:

$$\psi_{\text{sim_AAS}} = \frac{\dot{m}_{3a}ex_4 + \dot{m}_{cw}ex_{cw} + \dot{m}_{cc}ex_{\text{cool.re}} + \dot{m}_{hc}ex_{\text{hot.re}}}{\dot{m}_{1a}ex_1 + \dot{m}_{2a}ex_6 + \dot{m}_{cc}ex_{\text{cool.sup}} + \dot{m}_{hc}ex_{\text{hot.sup}}}, \quad (24)$$

$$\psi_{\text{sim_CRCS_AHU}} = \frac{\dot{m}_aex_4 + \dot{m}_{cw}ex_{cw} + \dot{m}_{cc}ex_{\text{cool.re}} + \dot{m}_{hc}ex_{\text{hot.re}} + \dot{m}_{chc}ex_{\text{ceil.re}}}{\dot{m}_aex_1 + \dot{m}_{cc}ex_{\text{cool.sup}} + \dot{m}_{hc}ex_{\text{hot.sup}} + \dot{m}_{chc}ex_{\text{ceil.sup}}}, \quad (25)$$

$$\psi_{\text{sim_HRCS_AHU}} = \frac{\dot{m}_aex_4 + \dot{m}_{cw}ex_{cw} + \dot{m}_{cc}ex_{\text{cool.re}} + \dot{m}_{chc}ex_{\text{ceil.re}}}{\dot{m}_aex_1 + \dot{m}_{cc}ex_{\text{cool.sup}} + \dot{m}_{chc}ex_{\text{ceil.sup}}}. \quad (26)$$

Rational ratios for different systems are shown as follows:

$$\psi_{\text{rat_AAS}} = \frac{\dot{m}_{1a}(ex_4 - ex_1) + \dot{m}_{2a}(ex_4 - ex_6)}{\dot{m}_{cc}(ex_{\text{cool.sup}} - ex_{\text{cool.re}}) + \dot{m}_{hc}(ex_{\text{hot.sup}} - ex_{\text{hot.re}}) + \dot{m}_{chc}(ex_{\text{ceil.sup}} - ex_{\text{ceil.re}})}, \quad (27)$$

$$\psi_{\text{rat_CRCS_AHU}} = \frac{\dot{m}_a(ex_4 - ex_1) + \dot{m}_a(ex_4 - ex_6)}{\dot{m}_{cc}(ex_{\text{cool.sup}} - ex_{\text{cool.re}}) + \dot{m}_{hc}(ex_{\text{hot.sup}} - ex_{\text{hot.re}}) + \dot{m}_{chc}(ex_{\text{ceil.sup}} - ex_{\text{ceil.re}})}, \quad (28)$$

$$\psi_{\text{rat_HRCS_AHU}} = \frac{\dot{m}_a(ex_4 - ex_1) + \dot{m}_a(ex_4 - ex_6)}{\dot{m}_{cc}(ex_{\text{cool.sup}} - ex_{\text{cool.re}}) + \dot{m}_{chc}(ex_{\text{ceil.sup}} - ex_{\text{ceil.re}})}. \quad (29)$$

The overall impact ratio for the cooling process is designed to present a system potential that combines the energetic analysis with exergetic analysis, as the ratio between the actual cooling energy output obtained for the air and water supplied and the total specific exergy consumed in a system, including the fan and pump consumption. In general, the electric pump and fan energy is 100% of the exergy because the main energy source of the fan and pump is electricity [10]. The overall cooling impact ratio (CIR) is defined as follows:

$$CIR_{\text{system}} = \frac{\dot{Q}_{\text{acc}}}{ex_{\text{e.c}}}, \quad (30)$$

$$CIR_{\text{AAS}} = \frac{\dot{Q}_{\text{acc_AAS}}}{\dot{m}_{cc}(ex_{\text{cool.sup}} - ex_{\text{cool.re}}) + \dot{m}_{hc}(ex_{\text{hot.sup}} - ex_{\text{hot.re}}) + \dot{m}_{chc}(ex_{\text{ceil.sup}} - ex_{\text{ceil.re}}) + P_{\text{fan.AHU}} + P_{\text{pump.AHU}}}, \quad (31)$$

$$CIR_{\text{CRCS_AHU}} = \frac{\dot{Q}_{\text{acc_CRCS_AHU}}}{\dot{m}_{cc}(ex_{\text{cool.sup}} - ex_{\text{cool.re}}) + \dot{m}_{hc}(ex_{\text{hot.sup}} - ex_{\text{hot.re}}) + \dot{m}_{chc}(ex_{\text{ceil.sup}} - ex_{\text{ceil.re}}) + P_{\text{pump.ceil}} + P_{\text{fan.AHU}} + P_{\text{pump.AHU}}}, \quad (32)$$

$$CIR_{\text{HRCS_AHU}} = \frac{\dot{Q}_{\text{acc_HRCS_AHU}}}{\dot{m}_{cc}(ex_{\text{cool.sup}} - ex_{\text{cool.re}}) + \dot{m}_{hc}(ex_{\text{hot.sup}} - ex_{\text{hot.re}}) + \dot{m}_{chc}(ex_{\text{ceil.sup}} - ex_{\text{ceil.re}}) + P_{\text{fan.Airbox}} + P_{\text{pump.ceil}} + P_{\text{fan.AHU}} + P_{\text{pump.AHU}}}, \quad (33)$$

where \dot{m}_{cc} is the cooling coil mass flow rate in kg/h, \dot{m}_{hc} is the heating coil mass flow rate in kg/h, \dot{Q}_{acc} is the actual cooling capacity, kJ/h, $ex_{\text{cool.sup}}$ is the specific exergy for cooling supply fluid in kJ/kg, $ex_{\text{cool.re}}$ is the specific exergy for cooling return fluid in kJ/kg, $ex_{\text{ceil.sup}}$ is the specific exergy for ceiling supply fluid in kJ/kg, $ex_{\text{ceil.re}}$ is the specific exergy for ceiling return fluid in kJ/kg, P_{pump} is the pump electricity in kJ/h, and P_{fan} is the fan electricity in kJ/h.

3. Results

3.1. Energy Performance of Systems

This study classified three main cooling systems and analyzed them numerically to evaluate the energy performance: an AAS, a CRCS with an AHU, and a HRCS with an AHU. Typically, an AAS uses a large amount air volume for cooling, and the air supplied reuses around 67% of the return air to reduce the cooling load. Compared to a typical radiant cooling system, an AAS consumes much volume space to supply a large air volume and has higher air pressure losses. A CRCS with an AHU can minimize the air volume supplied but also requires installing a hydronic pipe and a radiant panel. The HRCS connects a compact air convector to a radiant cooling panel hydronically in series. The convector can control the indoor air movement and the cooling capacity for the occupied zone efficiently. It can also reduce the condensation risks on the radiant panel surface and minimize the time delay in operating the chilled radiant cooling system in space.

This study used TRNSYS energy simulation software to analyze the cooling energy load in each building located in four main cities. Figure 7 presents the cooling load of the office room located in four cities in the summer season and the cooling capacities of the three systems. A CRCS has approximately the same cooling capacity as an AAS. However, it is limited to increasing the cooling output using lower-temperature supplied water under hot and humid surrounding conditions. The cooling capacities of an AAS and CRCS in 5–10 days of extreme weather conditions were insufficient to dominate the actual cooling loads; therefore, the systems needed additional cooling output to dominate the simulated cooling loads. Typically, an AAS can simply adjust the supplied airflow rate to increase the cooling output. However, a CRCS is limited to increasing the cooling output with lower temperature water supplied using a chilled radiant panel because the lower supplied water temperature causes moisture condensation risk on the surface of the radiant panel in an extreme hot and humid summer condition. The moisture condensation risk is the main limitation of the use of a chilled radiant cooling panel system in a hot and humid summer condition instead of using an AAS. However, the HRCS has a 20–30% relatively higher cooling capacity than the other two systems. The cooling output of the HRCS can be adjusted depending on the weather conditions using the heat exchanger capacity and fan speed of an airbox convector. The cooling output of the hybrid system, using the airbox increasing 1–2 °C of supplied water temperature and 1 m/s of air speed, is shown in Figure 7.

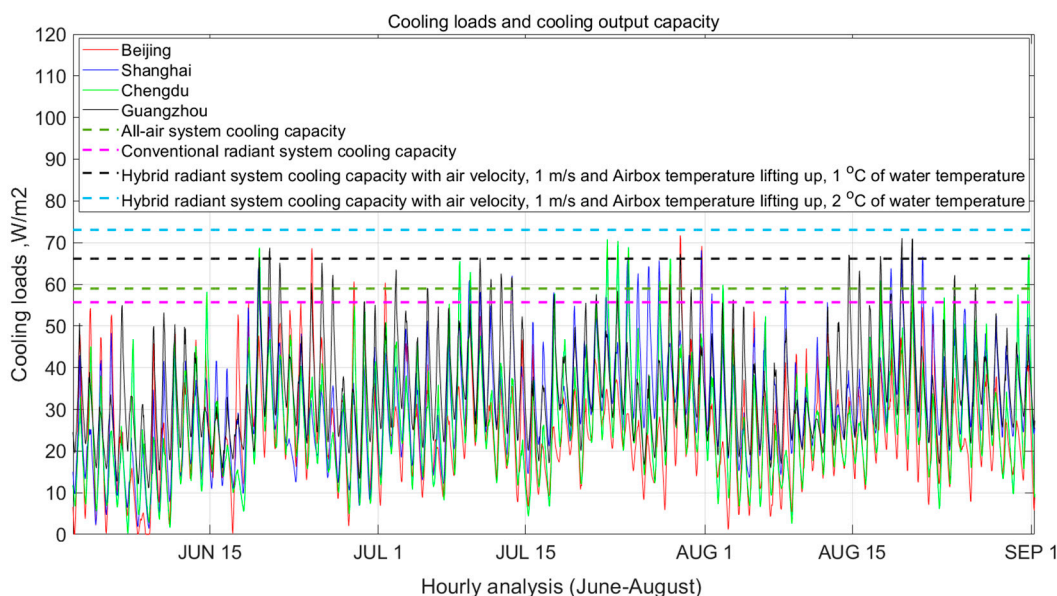


Figure 7. Cooling loads of the designed office room and the cooling capacities of the AAS, CRCS, and HRCS.

It can be concluded that the HRCS with an AHU adapted well to four different locations in the extreme hot and humid surrounding condition using even the same supply-water temperature, 18 °C, since the heat exchangers in the compact air convector and the mixed natural and mechanical forced convection effect enhanced the additional cooling potential outputs [43]. The occupants could simply turn on or turn off the airbox convector. Therefore, the indoor thermal comfort could be adjusted by the air convector's distributed air movement and directivity.

3.2. Exergy Analysis

In this study, the exergy performances of three cooling systems were analyzed and evaluated on the basis of the local historical hourly weather database of four cities in the summer season (June–August). The ambient environments are illustrated as shown in Figures 5 and 6 to determine the exergy performance of three cooling systems. Two main exergy efficiencies and the simple and rational ratios of the three systems were calculated and compared. Figure 8 presents the simple exergy efficiency ratio. There are no significant differences among the results. However, the simple exergy efficiency ratios of the HRCS and the CRCS were 2.72% and 2.20% higher than those of the AAS. Specifically, the ratio had the highest value in Beijing and the lowest value in Guangzhou because the Guangzhou climate in the summer was much more challenging than the weather conditions of the other cities.

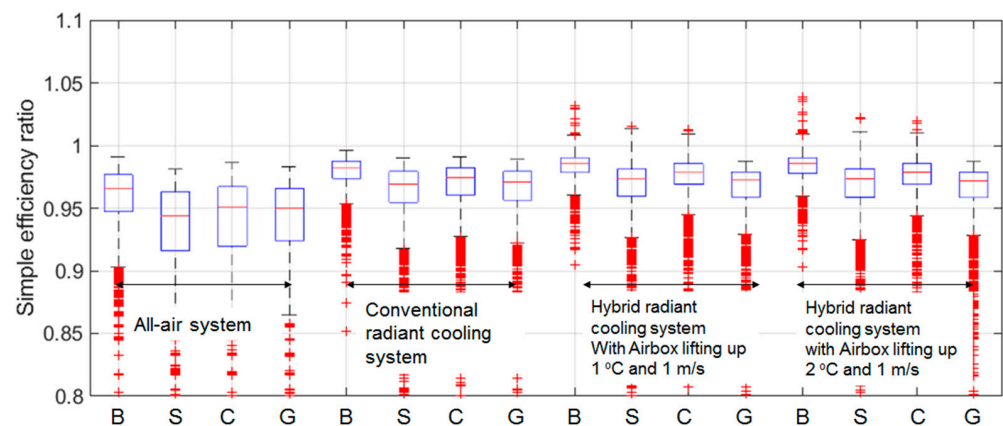


Figure 8. Simple exergy efficiencies of the three cooling systems in four cities: B—Beijing, S—Shanghai, C—Chengdu, and G—Guangzhou.

Figure 9 illustrates the rational exergy efficiencies of the three main systems. The HRCS with the AHU had the highest rational exergy efficiency compared with the other systems because the high-temperature cooling system maximized the actual exergy efficiency, especially in extreme weather conditions. The rational exergy efficiency ratio of the HRCS was 83%, 18% higher than the ratios of the AAS and the CRCS.

Moreover, the rational exergy efficiencies of the AAS were highly influenced by the ambient conditions compared with other radiant cooling systems, as shown in Figure 9. The maximum rational exergy efficiency in Beijing was much higher than that in Guangzhou, but the average value showed no significant differences because the temperature in Beijing deeply oscillates in the daytime and nighttime. Therefore, the ambient condition affected the efficiency of the AAS. It should be noted that the simple exergy efficiency ratio evaluates how close the process of the systems is to the ideal performance, and the rational exergy efficiency ratio presents how much potential the systems lose in generating specific outputs [56,60]. These two exergy efficiency ratios represent how the ambient environmental conditions affect the potentials of the systems.

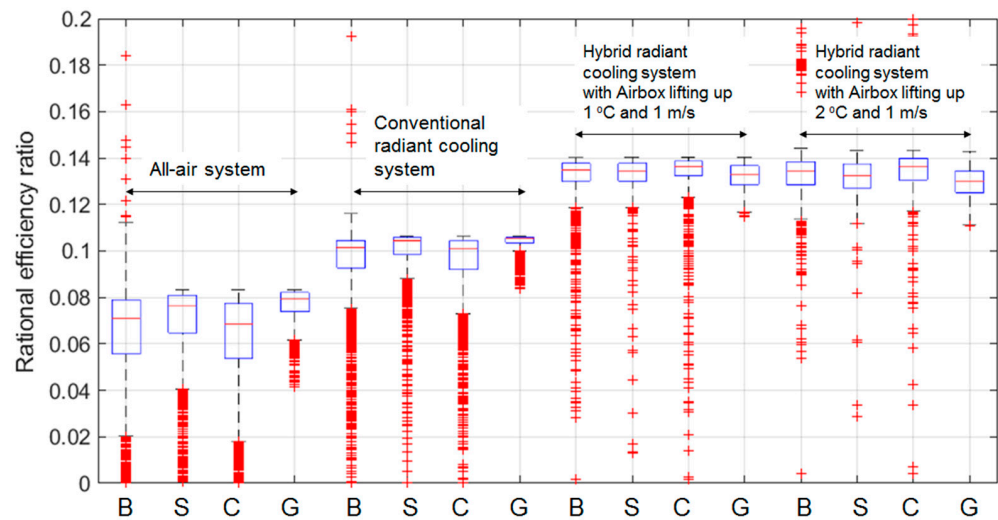


Figure 9. Rational exergy efficiencies of the three cooling systems in four cities: B—Beijing, S—Shanghai, C—Chengdu, and G—Guangzhou.

Figure 10 presents the overall cooling impact ratios (*CIRs*) of the three systems between the actual obtained energetic cooling potentials of the three systems and the overall exergy consumed in the systems combined with the exergetic consumption of the fan and pump. We concluded that the HRCS had the highest cooling output and relatively low exergy consumptions with respect to the other two systems. The overall *CIR* of the HRCS, with an airbox convector increasing 2 °C of the temperature and 1 m/s of the air velocity, was approximately 185% higher than that of the AAS, 8.5% higher than that of the CRCS, and 2% higher than that of the HRCS increasing 1 °C of the temperature and 1 m/s of the air velocity.

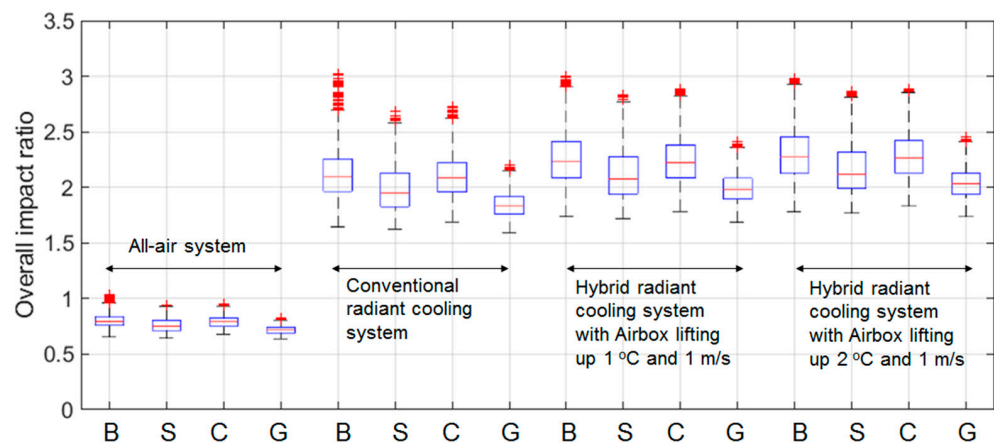


Figure 10. Overall impact ratio of the three cooling systems in four cities: B—Beijing, S—Shanghai, C—Chengdu, and G—Guangzhou.

Figure 11 illustrates the overall *CIR* using the weather conditions of four cities, Beijing, Shanghai, Chengdu, and Guangzhou. The high temperature and high humidity ratio of the ambient conditions affected the high exergy consumption. Therefore, these factors reduced the overall *CIR*. The impact ratio in Beijing had the highest value. The results varied more dramatically due to the high temperature differences between daytime and nighttime. However, the results at Guangzhou show that the relatively lower temperature differences between daytime and nighttime compared with other cities had less of an influence on the variation of the *CIR* results. The HRCS showed strong performance for the overall weather conditions compared with the other systems. It could maximize the potential for mild

conditions with a relatively lower temperature and humidity ratio difference between the ambient and indoor conditions.

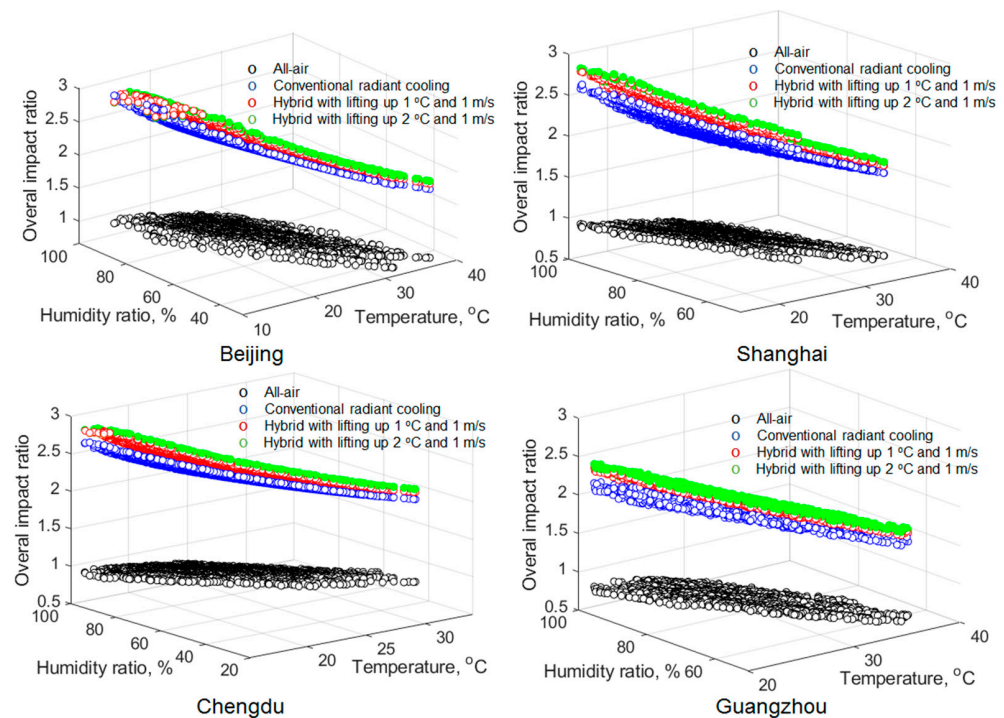


Figure 11. Overall impact ratio of three cooling systems in each city: upper left, Beijing; upper right, Shanghai; lower left, Chengdu; lower right, Guangzhou.

These numerical energetic and exergetic results indicate that the HRCS system with an AHU had better performance compared to the three cooling systems adapting to hot and humid conditions. This is because the HRCS could produce additional cooling output with a compact air convector and simply adjust the indoor thermal condition and humidity ratio using the airbox convector when a space had extra humidity gains. The low-exergy/high-temperature cooling source could improve the system performance and minimize the exergy destruction.

However, this study also had some limitations. The application potential of the radiant cooling systems is affected by different climatic conditions [61]. Therefore, the meteorological parameters in severe cold, cold, hot summer and cold winter, hot summer and warm winter, and temperate climatic zones should be evaluated considering the control strategies. Moreover, this study suggested an airbox convector to minimize moisture condensation risks on the surface of radiant cooling panels and to adjust airflow rates depending on the indoor thermal condition. However, the control strategy needs to be verified via experimental analysis [62,63]. The total energy and exergy analysis should also consider the initial construction and operating cost.

Nevertheless, further studies should consider evaluating the performance with actual experimental results to launch the system in extreme weather conditions successfully. Additionally, the thermal comfort in a room should be investigated using different cooling systems to verify the occupants' satisfaction in the future.

4. Conclusions

This study explored an energetic and exergetic analysis to evaluate the performance of three main air-cooling systems (AAS, CRCS, and HRCS) in an office building adapted to hot and humid summer conditions in four main cities in China: Beijing, Shanghai, Chengdu, and Guangzhou. Compared with a CRCS, the HRCS with an AHU could generate higher cooling outputs with an air convector due to an enhanced natural and mechanical forced convection effect. The system could minimize exergy losses in the process involved with

cooling in buildings. This study found that the HRCS had a higher overall impact ratio, and that lower temperature differences could minimize exergy destruction in the process of cooling and dehumidification. A summary of this study is described below.

- In the hot and humid summer season, the HRCS was the most efficient cooling strategy due to the extra cooling output provided by the compact convector and the relatively low exergy destruction in the cooling and dehumidification process with higher-temperature cooling sources.
- The HRCS released an additional 20–30% of cooling output, and it could adapt well in extreme hot and humid weather conditions.
- The comparison analysis using the four different weather datasets showed simple and rational exergy efficiency; as a result, the ambient condition, temperature, and humidity ratio significantly impacted the exergy efficiency ratio.
- The overall *CIR* of the HRCS with an airbox convector was approximately 185% higher than that of the AAS and 8.5% higher than that of the CRCS.
- The HRCS presented the most efficient characteristic in reducing the environmental impact and increasing the benefits compared with the AAS and CRCS in hot and humid summer conditions.

Author Contributions: Conceptualization, J.L. and M.K.K.; methodology, M.K.K.; software, M.K.K. and M.S.; validation, N.F., J.L. and M.K.K.; formal analysis, M.S. and M.K.K.; investigation, J.L. and M.S.; resources, J.L.; data curation, M.K.K.; writing—original draft preparation, J.L. and M.K.K.; writing—review and editing, J.L., M.S., N.F. and M.K.K.; visualization, M.S. and N.F.; supervision, M.K.K.; project administration, M.K.K.; funding acquisition, J.L. and M.K.K. All authors have read and agreed to the published version of the manuscript.

Funding: This work was funded by Natural Science Foundation of Shandong Province (ZR2021ME199, ZR2020ME211) and the Research Development Fund (RDF 15-02-32) of Xi'an Jiaotong—Liverpool University.

Institutional Review Board Statement: Not applicable.

Informed Consent Statement: Not applicable.

Data Availability Statement: Not applicable.

Acknowledgments: This work acknowledges the support of the Plan of Introduction and Cultivation for Young Innovative Talents in Colleges and Universities of Shandong Province, and Innovation Team of the Co-Innovation Center for Green Building of Shandong Province in Shandong Jianzhu University and Department of Built Environment in Oslo Metropolitan University.

Conflicts of Interest: The authors declare no conflict of interest.

Nomenclature

$c_{p,air}$	specific heat capacity value of air, kJ/(kg·K)
$c_{p,water}$	specific heat capacity of water, kJ/(kg·K)
$c_{p,vapor}$	specific heat capacity of water vapor, kJ/(kg·K)
h	enthalpy, kJ/kg
h_{fg}	specific enthalpy value of the vaporization of water, kJ/kg
\dot{m}	mass flow rate, kg/h
\dot{m}_{air}	mass flow rate of air, kg/h
\dot{m}_{water}	mass flow rate of water, kg/h
p	pressure, Pa
p_o	outdoor air pressure, Pa
p_{sat}	saturated water vapor pressure, Pa
P_{airbox}	airbox energy load, kJ/h
P_{fan}	fan electricity, kJ/h

P_{pump}	pump electricity, kJ/h
\dot{Q}	cooling load, kJ/h
\dot{Q}_{lat}	lateral cooling energy load, kJ/h
\dot{Q}_{sen}	sensible cooling energy load, kJ/h
\dot{Q}_{tot}	total cooling energy load, kJ/h
R_{air}	specific ideal gas constant, J/(kg·K)
T	temperature, K
T_{τ}	indoor air temperature at the time of τ , K
\dot{V}	air or water volumetric flow rate, m ³ /h
Greek letters	
Δ	difference or change in the specific parameter
η_{pump}	pump efficiency, %
η_{fan}	fan efficiency, %
τ	time
ν	specific volume for liquid water, m ³ /kg
ϕ	relative humidity, %
ψ_{sim}	simple or universal exergy efficiency, %
ψ_{rat}	rational and functional exergy efficiency, %
ω	humidity ratio, kg/kg
$\tilde{\omega}$	mole fraction ratio
Abbreviation	
AAS	all-air system
ACH	air change per hour, h ⁻¹
AHU	air handling unit
An	anergy, kJ/h
CIR	cooling impact ratio, %
COP	coefficient of performance
CRCS	conventional radiant cooling system
ex	specific exergy, kJ/kg
ex_{tot}	total specific exergy, kJ/kg
ex_{phys}	physical exergy, kJ/kg
ex_{chem}	chemical exergy, kJ/kg
HRCS	hybrid radiant cooling system
HVAC	heating, ventilation, and air-conditioning
Subscripts	
1, 2, 3, 4	process number presented in the Figures 1–3
1a, 2a, 3a	air mass flow in the process number presented in the Figures 1–3
a(ir)	air
c	cooling
acc	actual cooling capacity
cc	cooling coil
ceil	ceiling
ceil.re	ceiling return
ceil.sup	ceiling supply
chc	chilled ceiling
cool	cooling
cool.re	cooling return
cool.sup	cooling supply
cooling and dehum	cooling and dehumidification process for the systems
cw	condensed water
chem	chemical
desired.out	desired outdoor air
e.c.	energy consumption
hc	heating coil
hot.sup	hot water supply

hot.re	hot water return
in	inlet
input	exergy or anergy input
lat	latent cooling load
max	maximum
mix.air	mixed air
o	outdoor
out	outlet
p	pressure
phys	physical
rat	rational ratio
re	return
rec	re-circulated
reheat	reheated air
sat	saturated
sen	sensible cooling load
sim	simple
sup	supply
sup.air	supply air
sup.water	supply water
tot	total
w	water

References

- De la Rue du Can, S.; Price, L. Sectoral trends in global energy use and greenhouse gas emissions. *Energy Policy* **2008**, *36*, 1386–1403. [\[CrossRef\]](#)
- Andrić, I.; Koc, M.; Al-Ghamdi, S.G. A review of climate change implications for built environment: Impacts, mitigation measures and associated challenges in developed and developing countries. *J. Clean. Prod.* **2019**, *211*, 83–102. [\[CrossRef\]](#)
- Zhu, X.; Liu, J.; Zhu, X.; Wang, X.; Du, Y.; Miao, J. Experimental Study on Operating Characteristic of a Combined Radiant Floor and Fan Coil Cooling System in a High Humidity Environment. *Buildings* **2022**, *12*, 499. [\[CrossRef\]](#)
- Liu, J.; Ren, J.; Zhang, L.; Xie, X.; Kim, M.K.; Zhang, L. Optimization of Control Strategies for the Radiant Floor Cooling System Combined with Displacement Ventilation: A Case Study of an Office Building in Jinan, China. *Int. J. Archit. Eng. Technol.* **2019**, *6*, 33–48.
- Bejan, A. Entropy Generation Minimization, Exergy Analysis, and the Constructal Law. *Arab. J. Sci. Eng.* **2013**, *38*, 329–340. [\[CrossRef\]](#)
- Liu, J.; Xie, X.; Qin, F.; Song, S.; Lv, D. A case study of ground source direct cooling system integrated with water storage tank system. *Build. Simul.* **2016**, *9*, 659–668. [\[CrossRef\]](#)
- Lohani, S.P.; Schmidt, D. Comparison of energy and exergy analysis of fossil plant, ground and air source heat pump building heating system. *Renew. Energy* **2010**, *35*, 1275–1282. [\[CrossRef\]](#)
- Kazanci, O.B.; Shukuya, M. A theoretical study of the effects of different heating loads on the exergy performance of water-based and air-based space heating systems in buildings. *Energy* **2022**, *238*, 122009. [\[CrossRef\]](#)
- Shukuya, M. Exergetic approach to the understanding of built environment—State-of-the-art review. *Jpn. Archit. Rev.* **2019**, *2*, 143–152. [\[CrossRef\]](#)
- Shukuya, M. Exergy concept and its application to the built environment. *Build. Environ.* **2009**, *44*, 1545–1550. [\[CrossRef\]](#)
- Kim, M.K.; Leibundgut, H.; Choi, J.H. Energy and exergy analyses of advanced decentralized ventilation system compared with centralized cooling and air ventilation systems in the hot and humid climate. *Energy Build.* **2014**, *79*, 212–222. [\[CrossRef\]](#)
- Pires, L.; Silva, P.D.; Castro Gomes, J.P. Experimental study of an innovative element for passive cooling of buildings. *Sustain. Energy Tech.* **2013**, *4*, 29–35. [\[CrossRef\]](#)
- Ren, J.; Liu, J.; Zhou, S.; Kim, M.K.; Song, S. Experimental study on control strategies of radiant floor cooling system with direct-ground cooling source and displacement ventilation system: A case study in an office building. *Energy* **2022**, *239*, 122410. [\[CrossRef\]](#)
- Kim, M.K.; Leibundgut, H. A case study on feasible performance of a system combining an airbox convector with a radiant panel for tropical climates. *Build. Environ.* **2014**, *82*, 687–692. [\[CrossRef\]](#)
- Manjunath, K.; Kaushik, S.C. Second law thermodynamic study of heat exchangers: A review. *Renew. Sustain. Energy Rev.* **2014**, *40*, 348–374. [\[CrossRef\]](#)
- Yucer, C.T.; Hepbasli, A. Thermodynamic analysis of a building using exergy analysis method. *Energy Build.* **2011**, *43*, 536–542. [\[CrossRef\]](#)
- Hürdoğan, E.; Buyükalaca, O.; Hepbasli, A.; Yilmaz, T. Exergetic modeling and experimental performance assessment of a novel desiccant cooling system. *Energy Build.* **2011**, *43*, 1489–1498. [\[CrossRef\]](#)

18. Torio, H.; Schmidt, D. Development of system concepts for improving the performance of a waste heat district heating network with exergy analysis. *Energy Build.* **2010**, *42*, 1601–1609. [[CrossRef](#)]
19. Meggers, F.; Ritter, V.; Goffin, P.; Baetschmann, M.; Leibundgut, H. Low exergy building systems implementation. *Energy* **2012**, *41*, 48–55. [[CrossRef](#)]
20. Meggers, F.; Pantelic, J.; Baldini, L.; Saber, E.; Kim, M.K. Evaluating and adapting low exergy systems with decentralized ventilation for tropical climates. *Energy Build.* **2013**, *67*, 559–567. [[CrossRef](#)]
21. Schmidt, D. Low exergy systems for high-performance buildings and communities. *Energy Build.* **2009**, *41*, 331–336. [[CrossRef](#)]
22. Torio, H.; Angelotti, A.; Schmidt, D. Exergy analysis of renewable energy-based climatisation systems for buildings: A critical view. *Energy Build.* **2009**, *41*, 248–271. [[CrossRef](#)]
23. Zhang, L.; Fang, H.; Wang, W.; Liu, J. Energy-saving analysis of ground source heat pump combined with floor radiant air conditioning system. *Procedia Eng.* **2017**, *205*, 4067–4073. [[CrossRef](#)]
24. Zhang, T.; Liu, X.; Tang, H.; Liu, J.; Jiang, Y. Exergy and entransy analyses in air-conditioning system part 1—Similarity and distinction. *Energy Build.* **2016**, *128*, 876–885. [[CrossRef](#)]
25. Zhang, L.; Liu, X.; Jiang, Y. Application of entransy in the analysis of HVAC systems in buildings. *Energy* **2013**, *53*, 332–342. [[CrossRef](#)]
26. Mosa, M.; Labat, M.; Lorente, S. Role of flow architectures on the design of radiant cooling panels, a constructal approach. *Appl. Therm. Eng.* **2019**, *150*, 1345–1352. [[CrossRef](#)]
27. Liu, J.; Li, Z.; Kim, M.K.; Zhu, S.; Zhang, L.; Srebric, J. A comparison of the thermal comfort performances of a radiation floor cooling system when combined with a range of ventilation systems. *Indoor Built Environ.* **2019**, *29*, 527–542. [[CrossRef](#)]
28. Niu, J.L.; Zhang, L.Z.; Zuo, H.G. Energy savings potential of chilled-ceiling combined with desiccant cooling in hot and humid climates. *Energy Build.* **2002**, *34*, 487–495. [[CrossRef](#)]
29. Jeong, J.-W.; Mumma, S.A. Ceiling radiant cooling panel capacity enhanced by mixed convection in mechanically ventilated spaces. *Appl. Therm. Eng.* **2003**, *23*, 2293–2306. [[CrossRef](#)]
30. Novoselac, A.; Srebric, J. A critical review on the performance and design of combined cooled ceiling and displacement ventilation systems. *Energy Build.* **2002**, *34*, 497–509. [[CrossRef](#)]
31. Jeong, J.W.; Mumma, S.A. Practical cooling capacity estimation model for a suspended metal ceiling radiant cooling panel. *Build. Environ.* **2007**, *42*, 3176–3185. [[CrossRef](#)]
32. Baldini, L.; Kim, M.K.; Leibundgut, H. Decentralized cooling and dehumidification with a 3 stage LowEx heat exchanger for free reheating. *Energy Build.* **2014**, *76*, 270–277. [[CrossRef](#)]
33. Su, M.; Liu, J.; Kim, M.K.; Wu, X. Predicting moisture condensation risk on the radiant cooling floor of an office using integration of a genetic algorithm-back-propagation neural network with sensitivity analysis. *Energy Built Environ.* **2022**, *in press*. [[CrossRef](#)]
34. Su, M.; Liu, J.; Zhou, S.; Miao, J.; Kim, M.K. Dynamic prediction of the pre-dehumidification of a radiant floor cooling and displacement ventilation system based on computational fluid dynamics and a back-propagation neural network: A case study of an office room. *Indoor Built Environ.* **2022**, *31*, 2386–2410. [[CrossRef](#)]
35. Hu, R.; Niu, J.L. A review of the application of radiant cooling & heating systems in Mainland China. *Energy Build.* **2012**, *52*, 11–19.
36. Rhee, K.N.; Olesen, B.W.; Kim, K.W. Ten questions about radiant heating and cooling systems. *Build. Environ.* **2017**, *112*, 367–381. [[CrossRef](#)]
37. Liu, J.Y.; Kim, M.K.; Srebric, J. Numerical analysis of cooling potential and indoor thermal comfort with a novel hybrid radiant cooling system in hot and humid climates. *Indoor Built Environ.* **2022**, *31*, 929–943. [[CrossRef](#)]
38. Yuan, Y.L.; Zhou, X.; Zhang, X. Numerical and experimental study on the characteristics of radiant ceiling systems. *Build. Res. Inf.* **2019**, *47*, 912–927. [[CrossRef](#)]
39. Liu, J.; Dalgo, D.A.; Zhu, S.; Li, H.; Zhang, L.; Srebric, J. Performance analysis of a ductless personalized ventilation combined with radiant floor cooling system and displacement ventilation. *Build. Simul.* **2019**, *12*, 905–919. [[CrossRef](#)]
40. Kim, M.K.; Liu, J.Y.; Cao, S.J. Energy analysis of a hybrid radiant cooling system under hot and humid climates: A case study at Shanghai in China. *Build. Environ.* **2018**, *137*, 208–214. [[CrossRef](#)]
41. Lim, H.; Kang, Y.-K.; Jeong, J.-W. Thermoelectric radiant cooling panel design: Numerical simulation and experimental validation. *Appl. Therm. Eng.* **2018**, *144*, 248–261. [[CrossRef](#)]
42. Krajčičk, M.; Šikula, O. The possibilities and limitations of using radiant wall cooling in new and retrofitted existing buildings. *Appl. Therm. Eng.* **2020**, *164*, 114490. [[CrossRef](#)]
43. Kim, M.K.; Leibundgut, H. Advanced Airbox cooling and dehumidification system connected with a chilled ceiling panel in series adapted to hot and humid climates. *Energy Build.* **2014**, *85*, 72–78. [[CrossRef](#)]
44. Kim, M.K.; Leibundgut, H. Evaluation of the humidity performance of a novel radiant cooling system connected with an Airbox convector as a low exergy system adapted to hot and humid climates. *Energy Build.* **2014**, *84*, 224–232. [[CrossRef](#)]
45. TRNSYS. *TRNSYS Transient System Simulation Tool*; Thermal Energy System Specialists, LLC: Madison, WI, USA, 2018.
46. Fang, H.; Wang, W.; Liu, J.; Zhang, L. Operation Analysis of a Compound Air Conditioning System using Measurement and Simulation. *Procedia Eng.* **2017**, *205*, 1454–1460. [[CrossRef](#)]
47. BS EN 1264-5:2008; Water Based Surface Embedded Heating and Cooling Systems. Heating and Cooling Surfaces Embedded in Floors, Ceilings and Walls. Determination of the Thermal Output European Committee for Standardization: Brussels, Belgium, 2008.

48. ISO 11855-6:2012; Building Environment Design—Design, Dimensioning, Installation and Control of Embedded Radiant Heating and Cooling Systems. International Organization for Standardization: Geneva, Switzerland, 2012.
49. ASHRAE 62.1 2013; Ventilation for Acceptable Indoor Air Quality. American Society of Heating, Refrigerating and Air-Conditioning Engineers, Inc.: Atlanta, GA, USA, 2013.
50. Jeong, J.W.; Mumma, S.A. Impact of mixed convection on ceiling radiant cooling panel capacity. *Hvac. R. Res.* **2003**, *9*, 251–257. [[CrossRef](#)]
51. Zhang, L.Z.; Niu, J.L. Indoor humidity behaviors associated with decoupled cooling in hot and humid climates. *Build. Environ.* **2003**, *38*, 99–107. [[CrossRef](#)]
52. Moran, M.J.; Shapiro, H.N. *Fundamentals of Engineering Thermodynamics*, 6th ed.; Wiley: Hoboken, NJ, USA, 2010.
53. Bejan, A. *Advanced Engineering Thermodynamics*, 4th ed.; John Wiley & Sons Inc.: Hoboken, NJ, USA, 2017.
54. Shukuya, M. *Exergy: Theory and Applications in the Built Environment*; Springer: London, UK, 2013.
55. Alpuche, M.G.; Heard, C.; Best, R.; Rojas, J. Exergy analysis of air cooling systems in buildings in hot humid climates. *Appl. Therm. Eng.* **2005**, *25*, 507–517. [[CrossRef](#)]
56. Shukuya, M.; Hammache, A. *Introduction to the Concept of Exergy—For a Better Understanding of Low-Temperature-Heating and High-Temperature-Cooling Systems*; VTT Technical Research Centre of Finland: Espoo, Finland, 2002.
57. Leoncini, L.; Baldi, M.G. Building Thermal Exergy Analysis. In *Mediterranean Green Buildings & Renewable Energy*; Sayigh, A., Ed.; Springer International Publishing: Cham, Switzerland, 2017; pp. 541–551.
58. Tsatsaronis, G. Thermoeconomic Analysis and Optimization of Energy-Systems. *Prog. Energy Combust.* **1993**, *19*, 227–257. [[CrossRef](#)]
59. Cornelissen, R. Thermodynamics and Sustainable Development. In *The Use of Exergy Analysis and the Reduction of Irreversibility*; University of Twente: Enschede, The Netherlands, 1997.
60. Morosuk, T.; Tsatsaronis, G. A new approach to the exergy analysis of absorption refrigeration machines. *Energy* **2008**, *33*, 890–907. [[CrossRef](#)]
61. Cui, M.; Liu, J.; Kim, M.K.; Wu, X. Application potential analysis of different control strategies for radiant floor cooling systems in office buildings in different climate zones of China. *Energy Build.* **2023**, *282*, 112772. [[CrossRef](#)]
62. Ren, J.; Liu, J.; Zhou, S.; Kim, M.K.; Miao, J. Developing a collaborative control strategy of a combined radiant floor cooling and ventilation system: A PMV-based model. *J. Build. Eng.* **2022**, *54*, 104648. [[CrossRef](#)]
63. Liu, J.; Zhu, X.; Kim, M.K.; Cui, P.; Zhu, S.; Kosonen, R. A Transient Two-dimensional CFD Evaluation of Indoor Thermal Comfort with an Intermittently-operated Radiant Floor Heating System in an Office Building. *Int. J. Archit. Eng. Technol.* **2020**, *7*, 62–87.

Disclaimer/Publisher’s Note: The statements, opinions and data contained in all publications are solely those of the individual author(s) and contributor(s) and not of MDPI and/or the editor(s). MDPI and/or the editor(s) disclaim responsibility for any injury to people or property resulting from any ideas, methods, instructions or products referred to in the content.